

Experimental and finite element studies of special-shape arch bridge for self-balance

Pengzhen Lu^{1*}, Renda Zhao¹ and Junping Zhang²

¹School of Civil Engineering, Southwest Jiaotong University, Chengdu, 610031, PR China

²School of Civil Engineering, Guangzhou University, Guangzhou, 510006, PR China

(Received July 30, 2007, Accepted January 5, 2010)

Abstract. Special-shape arch bridge for self-balance (SBSSAB) in Zhongshan City is a kind of new fashioned spatial combined arch bridge composed of inclined steel arch ribs, curved steel box girder and inclined suspenders, and the mechanical behavior of the SBSSAB is particularly complicated. The SBSSAB is aesthetic in appearance, and design of the SBSSAB is artful and particular. In order to roundly investigate the mechanical behavior of the SBSSAB, 3-D finite element models for spatial member and shell were established to analyze the mechanical properties of the SBSSAB using ANSYS. Finite element analyses were conducted under several main loading cases, moreover deformation and strain values for control section of the SBSSAB under several main loading cases were proposed. To ensure the safety and rationality for optimal design of the SBSSAB and also to verify the reliability of its design and calculation theories, the 1/10 scale model tests were carried out. The measured results include the load checking calculation, lane loading and crowd load, and dead load. A good agreement is achieved between the experimental and analytical results. Both experimental and analytical results have shown that the SBSSAB is in the elastic state under the planned test loads, which indicates that the SBSSAB has an adequate load-capacity. The calibrated finite-element model that reflects the as-built conditions can be used as a baseline for health monitoring and future maintenance of the SBSSAB.

Keywords: special-shape arch bridge; self-balance; model tests; finite element method; structural safety.

1. Introduction

Special-shape arch bridge for self-balance (SBSSAB) in Zhongshan City is major bridge over the Shizhi River, located on the No. 35 road in Zhongshan, Guangdong Province, China. The bridge is a critical project for the construction of the No. 35 road, lying within a leisure scene of Zhongshan District. Because of its geographical importance, the government of Zhongshan decided to build this bridge as a symbolic construction in Zhongshan and approved the special-shape arch bridge for self-balance proposed and designed by southwest Jiaotong University, in Chengdu, Sichuan Province, China (Zhang *et al.* 2003). The special-shape arch bridge for self-balance (SBSSAB) has a curved steel box girder deck construction consisting of single span with an overall length of 114 m and a width of 29.7 m, and the bridge has six-lane in two directions. In addition, the essence of its mechanics is a self equilibrium system; that is to say, the equilibrium system is made up of the

*Corresponding author, Ph.D., E-mail: pzh_lu@163.com

stiffness arch ribs, the bridge deck, and the inclined booms. Also, the stiffness arch ribs are designed to adopt the variable hexagonal cross-section with height from 1.5 m to 3.6 m and width from 1.8 m to 3.0 m, the bridge deck uses flat curved steel box girder, and the two transversal beams are set in the two ends of the stiffness arch ribs to enhance stability of the bridge. In terms of the self equilibrium system, bearing capacity of the bridge deck is achieved through the tensile force of the inclined booms and the bearing force of two transversal beams. Another characteristic of the bridge is that the stiffness arch rib itself is also a self equilibrium system. In addition, all inside and outside arch spans of the bridge are 100 m, but all rise-to-span and rise of the inside and outside arches are different. In the outside arch, the included angle between the outside arch and vertical plane is 13.5° with a rise-to-span ratio in the plane of $1/2.97$ and a rise of 37 m; in the inside arch, the included angle between the inside arch and vertical plane is 35.5° with a rise-to-span ratio in the plane of $1/3.65$ and a rise of 30 m. Inclined suspender spacing for inside and outside arch of the SBSSAB is all 5.0 m; there were 21 inclined suspenders for inside arch in total, there were 19 inclined suspenders for outside arch in total, and suspension points of the inclined suspenders lies at the curved steel box girder with interior diaphragms. This paper selects General Code for Design of Highway Bridges and Culvers-JTG D60 (2004) and Code for Design of Steel Structure-GB50017 (2003) as main design standard for the SBSSAB include design load and materials (Huang *et al.* 2004).

In addition, the special-shape arch bridge for self-balance (SBSSAB) is a multi-element spatial combined structure composed of two-piece inclined steel arch ribs, curved steel box girder and inclined suspenders. Although the span of the bridge is not very long, its structural form is special, and the weight of the main girder is connected and balanced by the inclined suspenders through optimal inclination of the arch rib, which is a crucial factor for the design of the SBSSAB. On the basis of self-balance structure mentioned above, the two main characteristics about the SBSSAB are as follows. First, the SBSSAB constitutes a multi-element spatial curve through two piece arch ribs

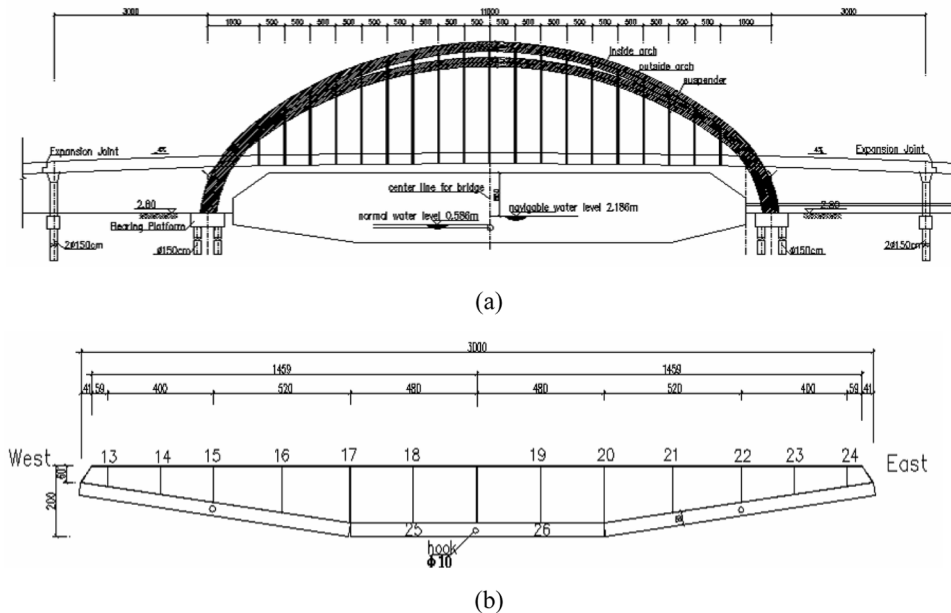


Fig. 1 General view of special-shape arch bridge for self-balance (a) elevation and (b) typical mid-span cross section of curved box girder deck

to establish self-balance for bridge structure, and there is almost no horizontal force for arch rib of the SBSSAB. Second, deformation for internal force of arch rib by structural dead weight offsets a part deformations from bridge deck loads include secondary dead loads and live loads.

In a word, the SBSSAB is a special-shape combined arch bridge with special geometry structures and complex mechanic behavior, and it is used in China and abroad for the first time. In order to ensure accurately the mechanical behavior of the bridge, 3-D finite element models for spatial member and shell were established to analyze the mechanical properties of the SBSSAB using ANSYS. Finite element analyses were conducted under several main loading cases, moreover deformation and strain values for control section of the SBSSAB under several main loading cases were proposed. To ensure the safety and rationality for optimal design of the SBSSAB and also to verify the reliability of its design and calculation theories, the 1/10 scale model tests were carried out, and results of the finite element analyses are in agreement with those of the tests. Fig. 1 shows the general view of the SBSSAB with schematic elevation, and typical cross section of curved steel box girder deck.

2. Experimental study

The scope of the experimental tests carried out at the University of Guangzhou was to investigate the mechanical behavior. The results of several main loading cases, such as the load checking calculation, lane loading and crowd load, and dead load were investigated.

2.1 Description of model design

To ensure the safety and rationality for mechanical behavior of bridge and also to verify the reliability of its design and calculation theories, the 1/10 scale model design was carried out. Also, the ratio of bridge original size to model size is 1/10 (Design and construction specification for steel-concrete composite structures 1992). According to the geometrical and physical similar principle, other similar ratios were presented. The main physical similar ratios include steel plate thickness (1/9), stress (9/10), mass (1/900), inertia moment (1/9000), elastic modulus (1:1), and displacement (9/100). Meanwhile, the gravity weight is adopted as loading, and its maximum load is 29.5t during the tests. Model of the bridge is shown in Fig. 2 (Han 2000).



Fig. 2 Scaled model of special-shape arch bridge for self-balance

2.2 Objectives and instrumentation of model tests

The fundamental objective of the mode static load tests on the newly constructed special-shape arch bridge for self-balance (SBSSAB) is to check if the bridge safety performance satisfies the design requirements and to determine if the bridge is allowed to go into service accordingly or not. More particular objective of the model tests include: (1) Finding out the mechanical behavior and load-carrying capacity under the planned static load conditions; (2) proving the accuracy and rationality of design theory to investigate the relationship for stiffness matching and internal force distribution between two piece arch ribs and curved steel box girders, end cross beam; (3) checking the quality and reliability of construction; (4) verifying the accuracy and rationality of design principle to facilitate the future design of similar types of bridges; (5) calibrating a three dimensional finite-element model to have a baseline model for further study of the bridge performance under other types of service load conditions; and (6) setting up the basic data for the health monitoring and future maintenance of the bridge.

The main measurement tasks of the load tests on the special-shape arch bridge for self-balance include the deck deflections, arch rib deformations, and strains (stresses) of the key structural parts under the planned test loading. One of the important features of special-shape arch bridge for self-balance is that the self-weight is dominant. The pretensions in the inclined suspenders control the

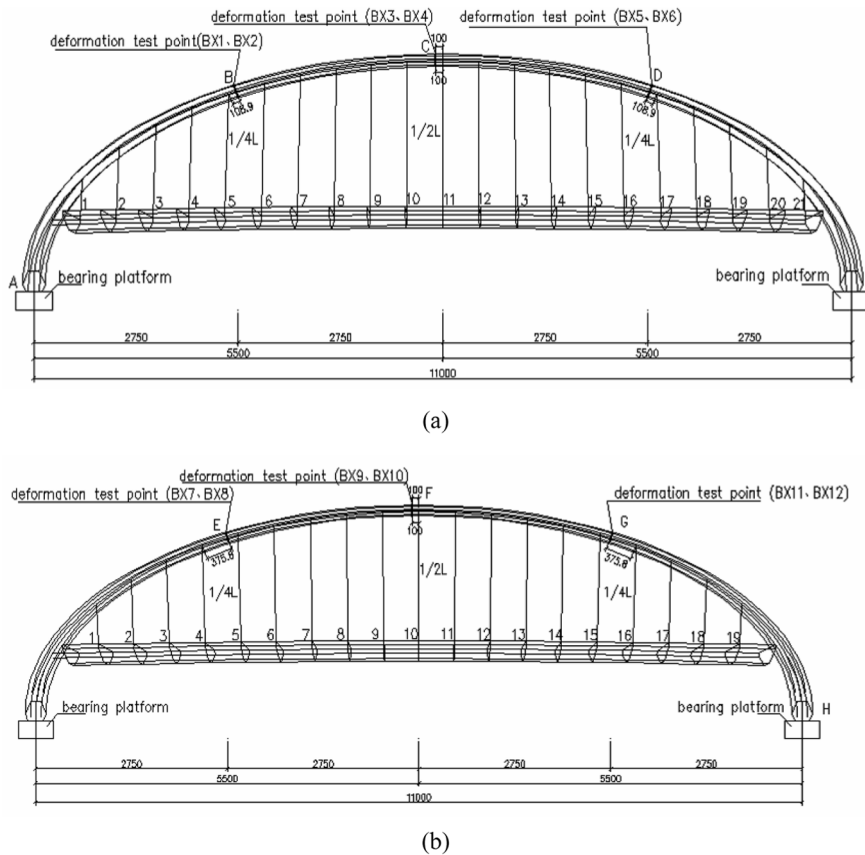


Fig. 3 Section for the deformation and strain test of arch rib (a) inside and (b) outside arch rib

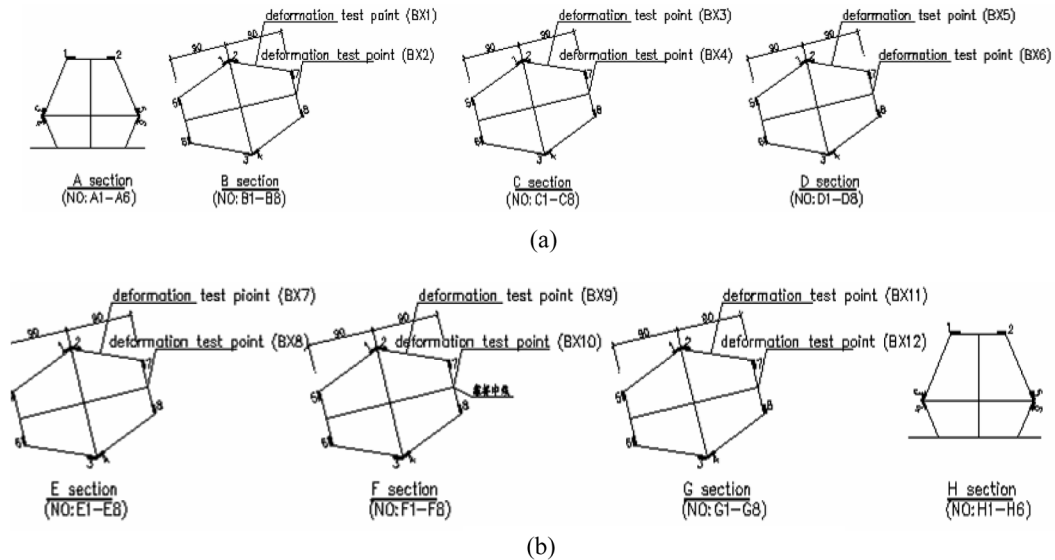


Fig. 4 Point layout for control section of arch rib (a) inside arch rib and (b) outside arch rib

internal force distribution and the bridge deck profile. The initial equilibrium configuration of special-shape arch bridge for self-balance is, therefore, the final elevation of the bridge deck, which is the bridge initial equilibrium position due to dead load, and tension forces in the inclined suspenders. The initial equilibrium configuration is important in special-shape arch bridge for self-balance since it is a starting position to perform the succeeding analysis. Just before the load tests, the as-built elevation of the bridge deck was surveyed by using the precision leveling instruments.

To measure the deflection of arch rib, three control sections for both arch ribs of the special-shape arch bridge for self-balance were used as shown in Fig. 3. Each section had 4 key points, and there were, in total, $4 \times 3 = 12$ deflection measurement stations including $1/4L$, $3/4L$, and $1/2L$ (L =span length) to take the data as show in Fig. 4 (B-D;F-H). At the same time, the arch ribs deflections were simultaneously surveyed by using the precision leveling instruments to supplement the deflection results. In addition, the curved steel box girders also have three control sections as shown in Fig. 5. Each section had 2 key points, and there were, in total, $3 \times 2 = 6$ deflection measurement stations including $1/4L$, $3/4L$, and $1/2L$ (L = span length) to take the data as show in Fig. 6 (Y, Z, U). As a result, there were, in total, 26 deflection measuring points instrumented in the model tests.

In order to study the stress responses of the arch rib and curved steel box girders under various load conditions, the strain measurements were implemented at seven critical sections along the bridge length. As for the arch ribs, they are sections A-H as shown in Fig. 2. Thirty strain gauges were instrumented at A, B, C, and D sections, whereas thirty strain gauges were instrumented at E, F, G, and H sections. As for the curved steel box girders, they are sections X, Y, Z, U, and V as shown in Fig. 4. Each section had 12 key points, and there were, in total, $5 \times 12 = 60$ strain gauges including two end section, $1/4L$, $3/4L$, and $1/2L$ (L = span length) to take the data as show in Fig. 5 (X-V). In addition, 44 and 40 stain gauges were instrumented on the cross beam and inclined suspenders, respectively, to check the corresponding responses under the planned loads. As a result, there were, in total, 216 strain gauges instrumented in the model tests.

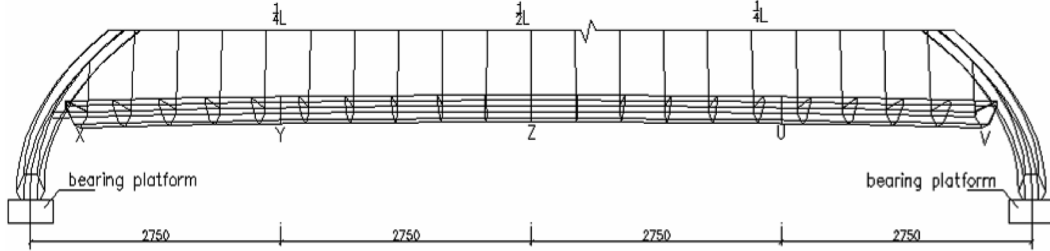


Fig. 5 Control section for deformation and strain of curved steel box girders

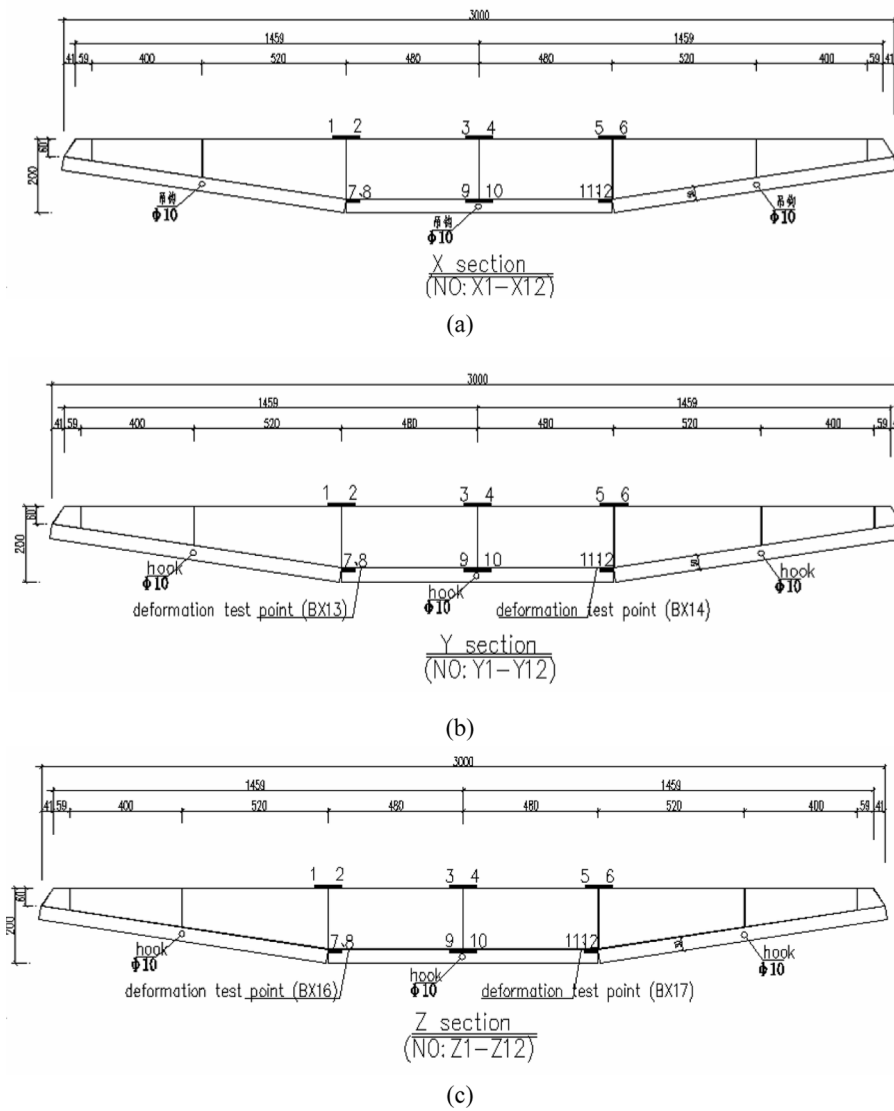


Fig. 6 Point layout for control section of curved steel box girders (a) X section, (b) Y section, (c) Z section, (d) U section, and (e) V section

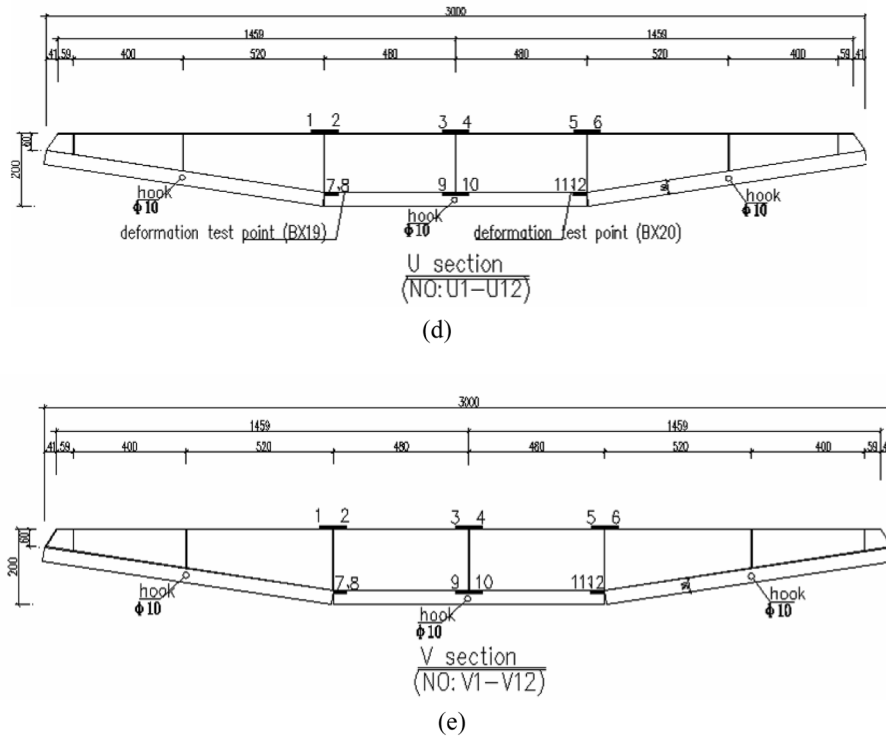


Fig. 6 Continued

2.3 Description of model tests

The main measurement tasks of the model tests on the special-shape arch bridge for self-balance include dead load, live load, and checking calculation, to simulate the design dead loads and live loads of the bridge (Truck-20 loads and Trailed-120 loads Specified in the Bridge Design Code of China). More follows operation principle of the model tests include: (1) according to grade, symmetry, and uniform; (2) using distributed load and each with 19.5 kg in the load tests ; (3) and adopting bridge deck heaped load and hanging basket loading. In addition, the applied model test loads should be, ideally, identical to the design live loads of the bridge. Due to the limitation of actual test conditions, however, the applied live loads and their distribution used in the tests might be different from those specified in the design codes. The applied test loads are normally designated by the static test load efficiency

$$\eta = \frac{S_d}{100S_t} \tag{1}$$

Where S_d = most critical value of static deformation or resultant force at the specified section of prototype bridge under the design loads; S_t = most critical value of static deformation or resultant force at the same specified section under the test loads; η = test load efficiency.

To fully understand the loading performance of such special-shaped arch bridge for self-balance, three different load cases were implemented during the model static load tests. All test load efficiency values are within 0.95~1.05, which demonstrates the validity of the statically loaded tests

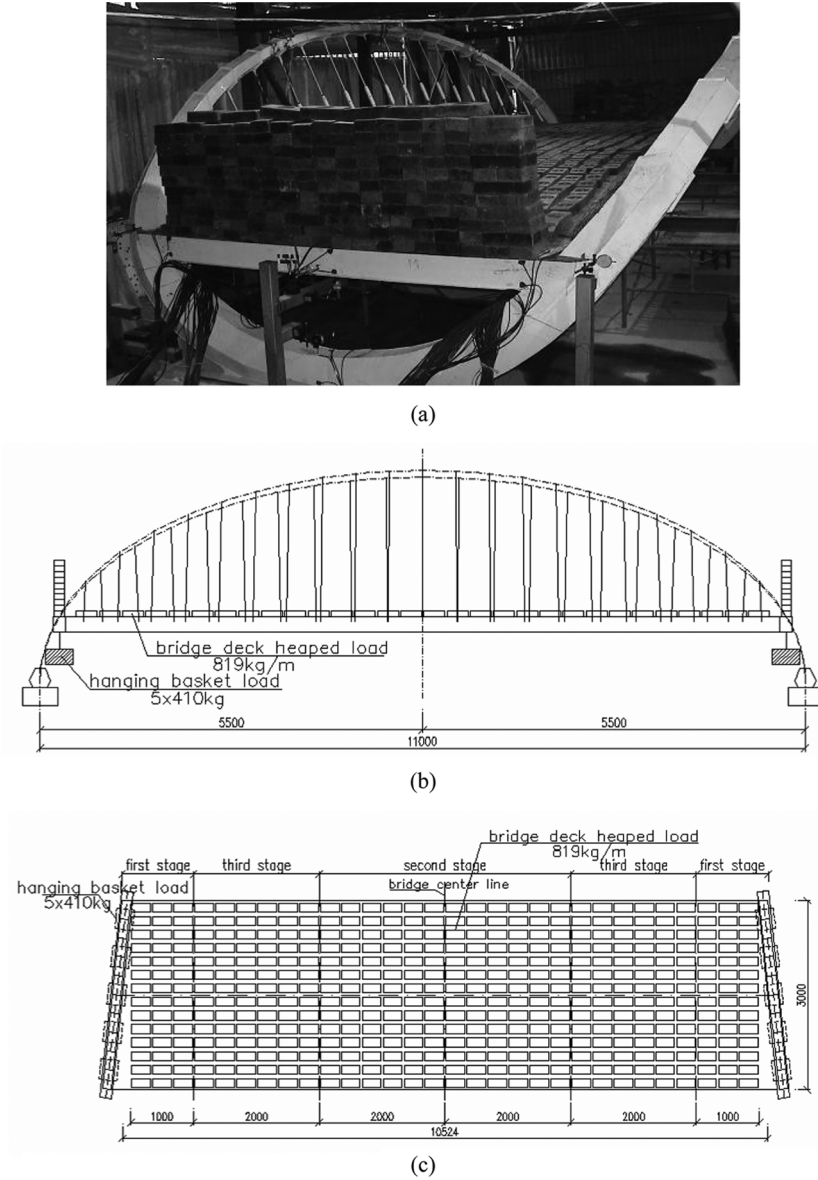


Fig. 7 Model test and loading plan for second period dead load (a) photo of model test, (b) elevation of Model Bridge loading plan, (c) plane of Model Bridge loading plan

Table 1 Weights of component parts of the the prototype bridge

| Structural member | One piece (t) | Total number | Total weight (t) |
|--|---------------|--------------|------------------|
| Longitudinal beam | 1322.3 | 1 | 1322.3 |
| Inside arch Pouring Concrete above bridge deck | 369.7 | 2 | 739.4 |
| Outside arch Pouring Concrete above bridge deck | 192 | 2 | 384 |
| Outside arch no Pouring Concrete above bridge deck | 56.5 | 2 | 113 |
| Inside arch no Pouring Concrete above bridge deck | 56.6 | 2 | 113.2 |
| Transversal beam | 120 | 2 | 240 |

on the bridge. The following three main loading cases were studied.

First, dead load, in another word, that is weights of the prototype special-shape arch bridge, as shown in Table 1, the dead load includes the first period dead load and second period dead load, and the applied modes about dead loads adopt uniform distribution. The dead load tests have two parts including first period dead load and second period dead load. 29119 kg and 16170 kg gravity weights were used in the period dead load and second period dead load, respectively, to check the corresponding responses under the planned dead loads. As a result, there were, in total, 45289 kg gravity weights in the dead load tests. In addition, distribution ways of the second period dead load include longitudinal beam in the arch rib range (816.94 kg/m) and concentrated force of the applied on corbel by approach (4000 kg). Loading plan and model test for second period dead load are shown in Fig. 7 (Fang *et al.* 2004).

Second, live load include lane loading and crowd load, and four different load cases were implemented during the live load tests. Live load arrangement mode is illustrated in Table 2. To simulate the design live loads of bridge (Tuck-20 and Trailer-120 loads specified in the Bridge Design Code of China), model test load arrangement mode is presented in Table 3. Loading plan and model test for live load are shown in Fig. 8 (Hou 2002).

Third, checking calculation load, the bridge design checking calculation load adopts Trailer-120 load (Trailer-120 load specified in the Bridge Design Code of China). To simulate the design

Table 2 Most disadvantageous arrangement of live load

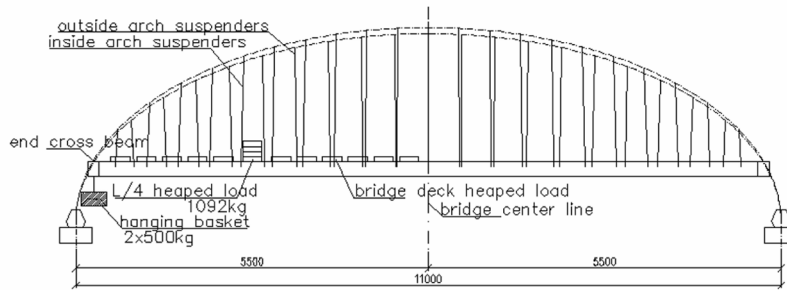
| Loading cases | Weight t/m | Concentrated force t | Concentrated force (corbel) (t) | Total weight (t) |
|--|---------------|-------------------------|------------------------------------|---------------------|
| Full loading of Full width (full-bridge) | 4.285 | 100 | 109 | 737.5 |
| Full loading of Full width (inside) | 2.935 | 50 | 75.83 | 469.3 |
| Full loading of Half cross section (outside) | 2.935 | 50 | 75.83 | 469.3 |
| Full loading of full width (1/2 the Length of Bridge) | 4.285 | 100 | 109 | 423.3 |

Table 3 Loading of the model by live load

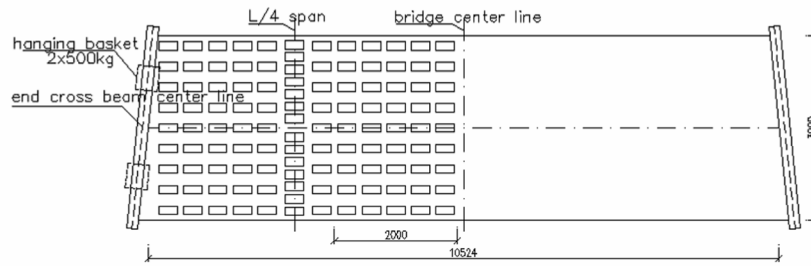
| Loading cases | Coverage of arch span kg/m | Concentrated force (corbel) (kg) | Concentrated force (kg) | Total weight (kg) |
|--|----------------------------------|--|-------------------------------|-------------------------|
| Full loading of Full width (full-bridge) | 428.5 | 1000.0 | 1090.0 | 7375 |
| Full loading of Half cross section of full-bridge (inside) | 293.5 | 500.0 | 758.3 | 4693 |
| Full loading of Half cross section of full-bridge (outside) | 293.5 | 500.0 | 758.3 | 4693 |
| Full loading of full width (1/2 the Length of Bridge) | 428.5 | 1000.0 | 1090.0 | 4233 |



(a)



(b)



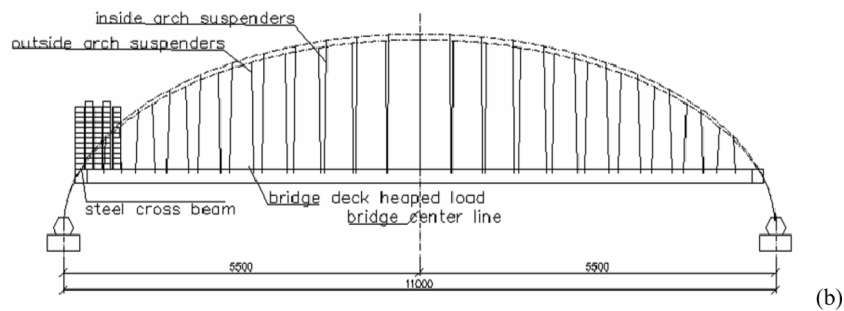
(c)

Fig. 8 Model test and loading plan for live load (a) photo of model test, (b) elevation of Model Bridge loading plan, (c) plane of Model Bridge loading plan

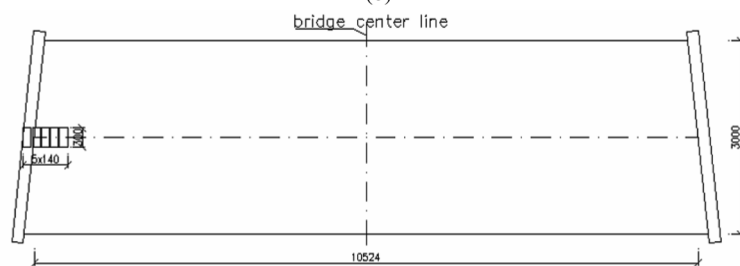
checking calculation load of the bridge, according to similar principle, model test checking calculation load uses 1200 kg. Model test checking calculation load include a trailer load applied in the middle span, a trailer load applied in the 1/4 location of the bridge span and a trailer load applied in the location between the end transversal beam and longitudinal beam. Loading plan and model test for checking calculation load are shown in Fig. 9 (Bathe and Jaeger 1992).



(a)



(b)



(c)

Fig. 9 Model test and loading plan for checking calculation load (a) photo of model test, (b) elevation of Model Bridge loading plan, (c) plane of Model Bridge loading plan

3. Finite element study

Creating a good three-dimensional model for special-shaped arch bridge for self-balance is not an easy task. Many different modeling strategies (i.e., which element types, how many degrees of freedom, etc.) are possible. The choice of strategy depends on the skill and experience of the analysts and on the intended application of the model. The established finite element model often requires achieving a balance between full bridge description and the degree of freedom. There is no unique way to conclude that the model developed by one is the best. Aimed at establishing a

baseline finite element model for the special-shaped arch bridge for self-balance, a full three-dimensional finite element model was developed in ANSYS (Kermani and Waldron 1993). The geometry and member details of the initial model are based on the design information and design blueprints of the bridge. The main structural members of the bridge are composed of inclined suspenders, inclined arch ribs, cross beam and curved steel box girders, all of which are described by different finite element types in current model. The main three kinds of element were adopted in the finite element models, including shell93 element, solid95 element and link10 element. Modeling of the inclined suspenders is possible in ANSYS by employing 3D tension-only truss elements (link10), and utilizing its stress-stiffening capability. With this element the stiffness is removed if the element goes into compression, thus simulating a slack suspender (Lu *et al.* 2006). The element is nonlinear and requires an iterative solution. Each inclined suspender is modeled by one element, which results in 40 tension-only truss elements in the model. The bridge deck upper plate, bottom plate, diaphragm plate, arch rib and cabinet base are modeled as the shell93 elements, which results in 34106 shell93 elements in the model (Mikkoal and Paavola 1980). All piers, platforms and concrete filled foe arch rib are modeled by the solid elements (solid95), which results in 24416 solid95 elements. The modeling of the bridge boundary conditions is very important. To the simplified analysis, in the current model, bridge bearings are modeled by a set of rigid link elements

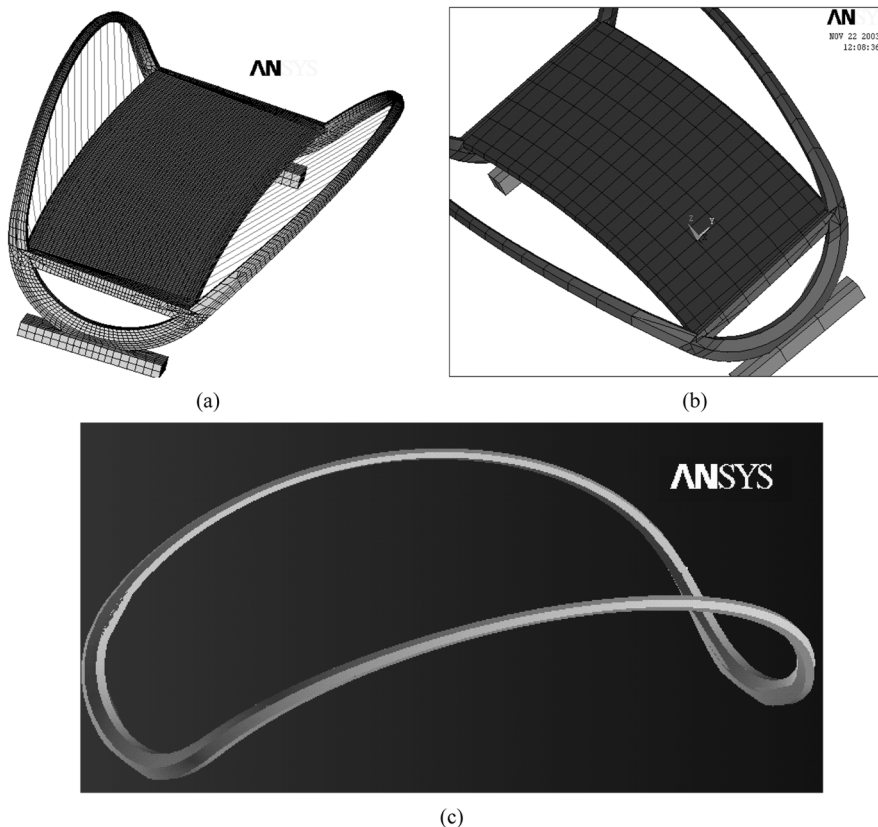


Fig. 10 Three-dimensional finite element model of the bridge (a) 3D view, (b) local view of curved steel box girders, (c) local view of arch ribs

connecting the superstructure and piers. To simulate the actual behavior, the bearings are simulated by coupling the corresponding translational and rotational degrees of freedom at both end nodes of the link elements. Subsequently, the developed full three-dimensional finite element model of the special-shaped arch bridge for self-balance is shown in Fig. 10. The model represents the bridge in its current as built configuration and structural properties (Paavoal 1993, Zhang *et al.* 2001).

4. Model tests and numerical analytical results

Among all three load cases, a comparison for analytical deflections of three load cases with those measured from field load tests is given in Table 4, are presented herein to illustrate the load-deflection behavior of bridge main structural parts (calculated deflections in the brackets). In addition, a comparison of analytical strains at the control section of bridge structure with those measured from model load tests is given in Table 5 (calculated strains in the brackets). According to the comparison between the calculated and measured results of the bridge main structural parts, both Table 4 and Table 5 clearly demonstrate a good correlation between the calculated and measured results of the bridge. It is observed that the initial equilibrium configuration of the Special-shape arch bridge for self-balance, as discussed previously, plays an important role in the calculation of

Table 4 Measured and calculated deflections (mm) at the control section of the model bridge

| Location | Dead load | Most adverse live load | Checking calculation |
|--------------------------|----------------|------------------------|----------------------|
| Inside arch rib (1/4L) | -5.06(-3.97) | 1.26(1.65) | 0.55(0.47) |
| Inside arch rib (1/2L) | -5.56(-4.39) | 1.56(1.71) | 0.85(0.55) |
| Outside arch rib (1/4L) | -9.68(-6.72) | -1.55(-1.02) | -0.90(-0.18) |
| Outside arch rib (1/2L) | -20.06(-15.11) | -4.51(-3.02) | -2.07(-0.98) |
| Longitudinal beam (1/4L) | -7.64(-5.35) | -1.91(-1.78) | -0.73(-0.38) |
| Longitudinal beam (1/2L) | -21.94(-17.43) | -3.89(-3.67) | -1.44(-1.45) |

Note: Taking vertical direction deflection as the comparison object; Taking upward vertical deflection as positive

Table 5 Measured and calculated strains ($\mu\epsilon$) at the control section of the model bridge

| Location | Dead load | Most adverse live load | Checking calculation |
|---------------------------------------|------------|------------------------|----------------------|
| Up edge of inside arch rib (L/4) | -479(-444) | -31(-92) | -33(-25) |
| Bottom edge of inside arch rib (L/4) | -322(-259) | -43(-44) | -62(-58) |
| Up edge of inside arch rib (L/2) | -383(-372) | -32(-21) | -8(-5) |
| Bottom edge of inside arch rib (L/2) | -807(-618) | -24(-36) | -40(-36) |
| Up edge of outside arch rib (L/4) | -556(-391) | -30(-42) | -52(-44) |
| Bottom edge of outside arch rib (L/4) | -383(-405) | -59(-65) | -85(-78) |
| Up edge of outside arch rib (L/2) | -547(-480) | -84(-96) | -78(-57) |
| Bottom edge of outside arch rib (L/2) | -457(-475) | -25(-36) | -32(-29) |
| Longitudinal beam (L/4) | -172(-140) | 32(24) | 19(16) |
| Longitudinal beam (L/2) | -195(-158) | -82(-101) | -216(250) |

control sections of the special-shape arch bridge for self-balance. Once the finite-element model was calibrated to match the as-built measured profile of the bridge, the model can predict a good control section deflection and strain. In addition, all of the deflections and strains observed in the entire testing programs were elastic. It is further shown that the control section deflections and strains can resume completely after all truck loads were removed. As a result, the load performance of the special-shape arch bridge for self-balance was shown to be satisfactory in terms of stiffness of bridge girders for self-balance. But there are also some differences. Main reasons will be put on the following three aspects. First, loading method of the model test is slightly different from Prototype Bridge. The loading mode of dead load adopts hanging basket and bridge deck heaped load, which is an approximate simulation for mass distribution of Prototype Bridge. Second, temperature variation has a great influence on the test results, and the finite element method cannot correctly simulate the effect of temperature variation. At the same time, external interference factors has great influence on the small strain test results, which results in the big error. Third, alignment and boundary condition of the bridge are slightly different from Prototype Bridge, however, according to the test results, deflection and strain values of the bridge is very sensitive to alignment change of the bridge arch rib (Moses *et al.* 1994).

5. Conclusions

Experimental and Finite Element Studies of Special-shape Arch Bridge for Self-balance are carried out in-depth. The main conclusions are obtained as follows:

(1) The deflection and strain values of the finite element analyses are in agreement with those of the tests under the planned loads, and the mechanical behavior of the bridge can be analyzed rightly by the finite element calculation model. Meanwhile, it was found that it is reasonable to adopt same model calculation prototype structure.

(2) There is a little maximal horizontal pushing force at the bearing platform top of Prototype Bridge under dead load or most adverse live load, and self-balance of the horizontal pushing force has been realized basically. As a result, pile foundation of the bridge was shown to be satisfactory in terms of strength.

(3) Different arch rib alignment is very sensitive to the mechanical behavior of the bridge. In the current model, arch rib alignment can be modified by tension suspenders or using concrete filled weight difference between inside arch rib and outside arch rib. In addition, deformation value for control section of the bridge is relatively great under first dead load, response (stress and deformation) of the arch rib under second dead load and live load can offset the impact under the first dead load, which shows that the key for the bridge design lies in the selection of reasonable arch rib alignment.

(4) Suspenders force of the bridge design under dead load or most adverse live load is a little different from model tests, but results of model tests is uniform. As a result, the designed suspenders parameters including suspenders structure, type, and initial tension are reasonable. Also, due to high order statically indeterminate mechanical properties for the bridge, different environment temperature and different foundation displacement for the bridge has great influence on the mechanical behavior of the bridge.

A few concluding discussions are offered here. Firstly, finite element analysis on the mechanical behaviors of the special-shaped arch for self-balance are rarely reported in the literature. This paper

demonstrated that finite element analysis is useful not only for dead load analysis but also for live load analysis. Secondly, according to the similar principle and the model test results under the planned load, it was found that stress for main members of the bridge has relatively large influences especially in the arch rib, the stress for arch rib control section from the bridge deck was close to 200 MPa and its maximum the stress for lower edge of longitudinal girder is 160 MPa, which results in deficiency for safety performance of the bridge. Also, hexagon-section of the bridge arch rib is not good for force situation, and it results in stress-focus phenomenon in the arch rib. Therefore, to increase stiffness of the bridge arch rib and decrease stress and deformation values, eliminating stress-focus phenomenon, in the current design, elliptical cross-section of the arch rib was adopted and plate thickness of the arch rib section was enlarged. Thirdly, the special-shaped arch bridge for self-balance located at the plane curves has two asymmetric arch ribs, arch rib alignment of the bridge is the most sensitive to the structural mechanical behavior, but design of the reasonable alignment is also very difficult. Therefore, in current model test or construction, elevation control plays an important role in the arch rib alignment and the main girder of the bridge. To realize design intension, construction detection, construction monitoring, and reasonable construction procedure are an essential way to ensure construction precision. Fourthly, stability behaviors and dynamic characteristics of the special-shaped arch bridge for self-balance are complicated to simulate in the ANSYS program, especially under moving loading. Therefore, the stability behaviors and dynamic characteristics of the bridge will be discussed in another paper. In addition, density for concrete filled of the bridge arch rib has great influence on each member internal force distribution and global stiffness. So, ultrasonic testing and chemical grouting are an essential measure to ensure construction quality.

References

- Bathe, B. and Jaeger, L.G. (1992), "Ultimate load test of slab girder bridge", *J. Struct. Eng-ASCE*, **114**(3), 1609-1625.
- Code for Design of Steel Structure-GB50017 (2003), China Architecture Building Press, Beijing. (in Chinese)
- General Code for Design of Highway Bridges and Culvers-JTG D60 (2004), China Comunication Press, Beijing. (in Chinese)
- Design and Construction Specification for Steel-concrete Composite Structures (1992), China Architectural Industry Press, Beijing. (in Chinese)
- Fang, I.K., Chen, C.R. and Chang, I.S. (2004), "Field static load test on Kao-Ping-His cable-stayed bridge", *J. Bridge Eng.*, **9**(6), 531-540.
- Huang, H.X., Shenton, H.W. and Chajes, M.J. (2004), "Load distribution for a highly skewed bridge: Testing and analysis", *J. Bridge Eng.*, **9**(6), 558-562.
- Hou, J.M. (2002), "Model test of the motive force characteristic of curved arched bridge", *The Journal of University of Chang An (natural science edition)*, **22**(3), 37-39.
- Han, L.H. (2000), *Concrete-filled Steel Tubular Structures*, Science Press, Beijing. (in Chinese)
- Kermani, B. and Waldron, P. (1993), "Analysis of continuous box beam bridges include in the effect of distorsion", *Comput. Struct.*, **16**(1), 427-739.
- Lu, P., Zhang, J. and Liu, A. (2006), "Structure analysis for Y-shape Bridge based on grillage theory", *Journal of Guangzhou University*, **5**(2), 67-72.
- Mikkoal, M.J. and Paavola, J. (1980), "Finite element analysis of box beams", *J. Struct. Eng-ASCE*, **106**(10), 1343-1357.
- Moses, F., Lebet, J.P. and Bez, R. (1994), "Applications of field testing to bridge evaluation", *J. Struct. Eng-ASCE*, **120**(6), 1745-1762.

- Paavoal, J. (1993), "A finite element technique for thin walled beams", *Comput. Struct.*, **144**(1/2), 159-175.
- Zhang, Q.W., Chang, T.Y.P. and Chang, C.C. (2001), "Finite-element model updating for the Kap Shui cable-stayed bridge", *J. Bridge Eng.*, **6**(4), 285-293.